View Article Online
View Journal

INORGANIC CHEMISTRY
FRONTIERS

Accepted Manuscript

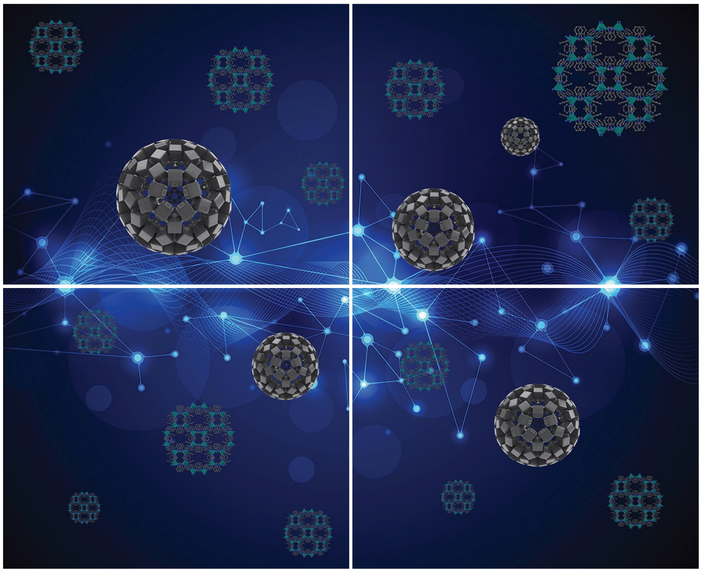

This article can be cited before page numbers have been issued, to do this please use: A. Tóth, B. Hajdu, Z. H. Nafaee, R. Sára Gyimesi, B. Gyurcsik, É. Hunyadi-Gulyás, J. G. Correia, J. Schell, T. T. Dang, K. Kato, A. Kawaguchi, L. Hemmingsen and A. Jancsó, *Inorg. Chem. Front.*, 2026, DOI: 10.1039/D6QI00876C.

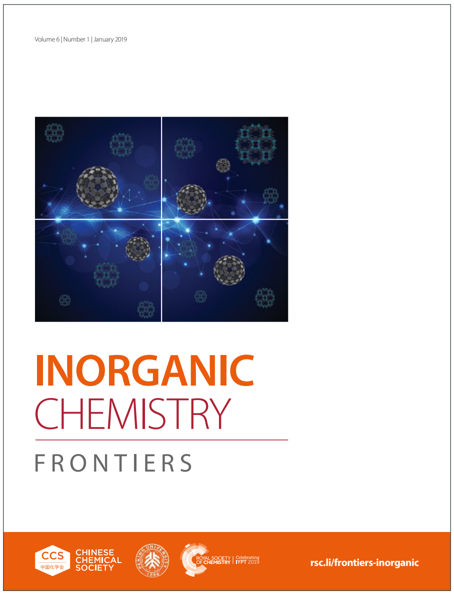

View Article Online
DOI: 10.1039/D6QI00876C

Received 00th January 20xx,
Accepted 00th January 20xx

DOI: 10.1039/x0xx00000x

Assessing the functional selectivity of an arsenic sensing protein *in vitro* and *in vivo*

Annamária Tóth,[a] Bálint Hajdu,[a,b] Zeyad H. Nafaee,[a,c] Réka Sára Gyimesi,[a] Béla Gyurcsik,[a] Éva Hunyadi-Gulyás,[d] Joao Guilherme Correia,[e,f] Juliana Schell,[e,g] Thanh Thien Dang,[g] Kohsuke Kato,[h] Atsushi Kawaguchi,[h] Lars Hemmingsen[b] and Attila Jancsó*[a]

The homodimeric bacterial ArsR proteins respond to As^{III} and Sb^{III}. Binding of the metalloids at coordination sites formed by three cyteine residues triggers an allosteric mechanism, leading to the release of the repressor ArsR protein from the operator DNA. Our study is focussed on the functional selectivity of ArsR from *Acidithiobacillus ferrooxidans* (AfArsR) both *in vitro* and *in vivo*. Binding of the inducers As^{III} and Sb^{III}, as well as non-cognate metal ions Hg^{II}, Pb^{II}, Cd^{II} and Zn^{II} to AfArsR were characterized by UV absorption titrations, ^{199m}Hg Perturbed Angular Correlation (PAC) of γ-rays spectroscopy, and Electrospray Ionization Mass Spectrometry (ESI-MS). The data indicate that metalloid binding at the two metalation sites is sequential. Correspondingly, Electrophoretic Mobility Shift Assays (EMSA) demonstrated that ca. 1.0 equivalent of As^{III} per protein dimer leads to a significant dissociation of the protein-DNA complex, suggesting that activation of the protein dimer requires the binding of only one As^{III}. Contrary to this, an Sb^{III}:AfArsR dimer concentration ratio higher than 1 was required to induce dissociation of the DNA from the DNA-protein complex. The divalent thiophilic metal ions bind strongly to the protein, but do not induce dissociation of the DNA-protein complex. This demonstrates that the inherent, molecular-level metalloid selectivity of AfArsR is not achieved via binding affinity differences. Interestingly, when combined with the inducer As^{III}, Hg^{II} was able to prevent the dissociation of the AfArsR dimer-DNA complex, however, this inhibiting effect of Hg^{II} was reversed by the addition of dimercaptosuccinic acid (DMSA). Selective As^{III}/Sb^{III} response of AfArsR was also observed *in vivo* in a bioreporter construct. The divalent metal ions, even Hg^{II}, did not compromise this effect, presumably due to the presence of competing thiol-containing Hg^{II}-binders in the cell, in analogy to the presence of DMSA *in vitro*. Experiments on mutant proteins confirmed that Cys95 and Cys96 are essential for and that C102 affects the protein function. Moreover, our data indicate that the His97Asp mutation also affects the metalloid response of the protein *in vivo*.

Introduction

ArsR metalloregulators play a key role in arsenic (and antimony) resistance in bacteria by controlling transcription[1–3] through a derepression mechanism. Members of the ArsR protein family form homodimers[1,4] that is required for DNA-binding and thus for the repression of transcription.[4–8] The homodimeric ArsR protein is bound to the operator/promoter region of the *ars* operon (DNA). Metalloid binding to ArsR exerts a negative allosteric effect on the stability of the repressor protein-DNA complex, leading to dissociation of ArsR from the regulated DNA and ultimately to the transcription of the regulated genes.[1]

Across the ArsR/SmtB family, the three cysteine residues that constitute the As^{III} binding sites are located in different regions of the proteins.[1] The C32, C34 and C37 residues in EcArsR (*E. coli*) and in the R773 plasmid-related ArsR (of *E. coli*) are part of the DNA-binding domain and constitute an intradomain α3 type site.[1,9] The three coordinating cysteines, C95, C96 and C102, are also located in the same monomer in AfArsR (*A. ferrooxidans*), making up a α5 type site.[9] SpArsR, identified from *S. putrefaciens*, has a similar structure to that of AfArsR, however, it lacks a third coordinating residue that would correspond to C102 in AfArsR and displays only two Cys residues near its C-terminus for a two-coordinate binding site with a selectivity for MeAs^{III}.[10] A third type of metalloid binding sites was identified in CgArsR (*C. glutamicum*), formed by the C15 and C16 residues from one monomer and the C55' cysteine from the other monomer in a non-typical interdomain α2-N site.[9] Finally, a very recent study described a possibly new type of As^{III} and MeAs^{III} responsive ArsR-family transcriptional regulator with 6 cysteine

---

[a] Department of Molecular and Analytical Chemistry, University of Szeged, Dóm tér 7-8. H-6720 Szeged, Hungary
[b] Department of Chemistry, University of Copenhagen, Universitetsparken 5, 2100 København Ø, Denmark
[c] College of Pharmacy, University of Babylon, Hillah 51001, Iraq
[d] Proteomics Research Group, Core Facility, Biological Research Centre, HUN-REN, Temesvári krt. 62, H-6726, Szeged, Hungary
[e] European Organization for Nuclear Research (CERN), CH-1211 Geneva, Switzerland
[f] Centro de Cięncias e Tecnologias Nucleares, Departamento de Engenharia e Cięncias Nucleares, Instituto Superior Técnico, Universidade de Lisboa, 2695-066 Bobadela LRS, Portugal
[g] Institute for Materials Science and Center for Nanointegration Duisburg-Essen (CENIDE), University of Duisburg-Essen, 45141 Essen, Germany
[h] Department of Infection Biology, Institute of Medicine, University of Tsukuba, 1-1-1 Tennodai, Tsukuba, 305-8575, Japan

† Footnotes relating to the title and/or authors should appear here.

Supplementary Information available: [details of any supplementary information available should be included here]. See DOI: 10.1039/x0xx00000x

View Article Online
DOI: 10.1039/D6QI00876G

residues (3×2 in nearby positions).[11] Based on site directed mutagenesis it was reported that only C41, C80 and C82, and C41 and C82 from the same chain are required for the protein to retain its responsiveness to As^{III} and MAs^{III}, respectively.[11] Despite the different spatial locations of the Cys units, the local structures of these metalloid sites are highly similar, shaping a trigonal pyramid around the As^{III} centres. Interestingly, the superimposition of the crystal structures of As^{III}-AfArsR and As^{III}-CgArsR reflects that the congruent metal sites are placed very similarly in the 3D structures of these different types of effector binding sites.[9]

Clearly, it is interesting to elucidate how ArsR proteins achieve selectivity for the cognate effector trivalent metalloids. We have approached this problem in a recent study, using the metalloid binding oligopeptide fragment of the AfArsR protein, to compare the As^{III} and Hg^{II} binding features.[12] Our data suggested that the peptide in itself is disordered, while binding of As^{III} locks it into a (or a few) well defined structure(s) with a trigonal pyramidal AsS$_3$ metalloid binding site. Hg^{II} also binds to the three cysteine residues, but in a distorted trigonal planar structure, and the peptide remains significantly disordered.[12]

Surprisingly, beyond our peptide mimicking efforts, no detailed *in vitro* study on the functional selectivity of ArsR proteins has been reported so far. *In vitro* studies have focussed mainly on the binding of different metalloid forms (As^{III}, As^{V}, Sb^{III}, Sb^{V}, MeAs^{III}, PhAs^{III}) to the proteins and their impact on the repressor-DNA complex,[10,13–17] but other potentially efficiently coordinating metal ions were very rarely involved in these studies (except for Bi^{III} [13] and Cd^{II} [15]). A gel mobility shift assay, investigating the As^{V}, As^{III}, Sb^{III} and Bi^{III} promoted dissociation of *E. coli* R773 ArsR from a specific DNA, containing the *ars* promoter, indicated that As^{V} is not a natural inducer of the regulator and Bi^{III} was also significantly less efficient than As^{III} and Sb^{III}.[13] In addition, As^{III}- and Sb^{III}-binding affinities were reported for some of the investigated ArsR proteins, such as *E. coli* R773 ArsR,[14] AfArsR[15], CgArsR[16] and CviArsR.[17]

The interaction of ArsR proteins with their effectors has been investigated under cellular conditions by bioreporter systems, using a reporter gene positioned within the *ars* operon. Various signalling proteins (encoded by the reporter gene) were applied in these studies, most commonly the green,[18–23] yellow,[24] or the mCherry[25] fluorescent proteins, the luciferase enzyme[21,25,26] for luminescence detection, or the β-galactosidase enzyme,[21,27,28] which produces electrochemical or colour signals by cleaving a designed substrate. Other sensors detect As^{III}-induced conformational change of ArsR based on fluorescence resonance energy transfer[29,30] or via altered fluorescence properties[31] as a consequence of the conformational change of the ArsR protein upon As^{III} binding. These constructs were developed and optimized for As^{III} detection in analytical samples. Most of them displayed significant signal induction in the presence of As^{III} and Sb^{III} as compared to the non-treated samples, while negligible signal enhancement was observed for other metal ions.[18–20,23,25,26,29] Nevertheless, further efforts are needed to improve the selectivity of the As^{III} biosensors through smart, engineered genetic logic circuits.[32]

With this work we advance from AfArsR peptide model studies to the actual protein and compare the binding of different metalloids and metal ions to this metalloregulator. The selection of the investigated non-cognate metal ions was based on coordination/bioinorganic chemistry considerations. All three divalent ions from group 12 (Zn^{II}, Cd^{II}, Hg^{II}) bear a certain level of thiophilic character, with an increasing affinity to thiolate donors from Zn^{II} to Hg^{II}. Zn^{II} is an essential metal ion, whereas Cd^{II} is highly toxic, nevertheless, both display a preference for coordination numbers over 3. Thiolate-rich metal sites are typical in metalloregulators responding to Zn^{II} (such as Zur[33]) and Cd^{II} (such as CadC[34]). Hg^{II} is known to prefer a bis-thiolate coordination environment[35] but can easily adopt tris-thiolate coordination in a trigonal planar geometry, as exemplified by MerR,[36] being notably different from the trigonal pyramidal environment around the metalloids dictated by their stereochemically active lone pair.[37] The main group metal ion Pb^{II} shows similarities to As^{III}/Sb^{III} with regard to its preference for tris-thiolate coordination (see e.g. the Pb^{II}-centre in PbrR[38]), as well as the usual hemidirected geometry in low-coordination Pb^{II}-structures owing to the stereochemically active lone pair,[37] but displays a lower (+2) charge.

We also explore the influence of the metalloids and the selected non-cognate metal ions on the interaction of AfArsR with its DNA target (see Scheme 1) by correlating the results of *in vitro* experiments (UV-absorbance, perturbed angular correlation of γ-rays spectroscopy and electrophoretic mobility shift assay) with *in vivo* data of I-Block bioreporter assays.[39] Such comparison may shed light on how significantly the different protein binding affinities and coordination geometry preferences may dictate the selection of the proper effector by the AfArsR protein. Scheme 1 provides a simple overview on the investigated metalloid regulation process, highlighting the previously explored details and the aims of the present work.

Results and discussion

Monitoring the metal(loid) interaction with AfArsR

The His-tagged AfArsR protein, identical to that crystallized in its As^{III}-bound form in an earlier study,[9] was successfully overexpressed and purified. Protein samples were titrated by solutions of As^{III}, Sb^{III} and divalent transition metal ions, with an aim to monitor the binding of these ions via evolution of thiolate to M^{III}/M^{II} LMCT bands in the wavelength range of ca. 200-360 nm.[12,40–44] The absorbance increase observed along with the increasing concentration of Hg^{II} or Pb^{II} up to two metal ion equivalents per protein dimer molecules clearly follows a linear trend (see Fig. 1 and Fig. S2A) indicating very efficient metal ion binding and a complete metalation at both metal sites of the protein dimer. Electrospray Ionization Mass Spectrometry (ESI-MS) spectra recorded in samples with increasing Hg^{II}:AfArsR concentration ratios support this conclusion (Fig. S3C). A linear trend in the change of absorbances was observed up to 1.5 equivalent of Cd^{II} per AfArsR dimer (Fig. S2B) beyond which the recorded spectra showed a gradual baseline increase, pointing to the formation of aggregates or precipitate.

View Article Online
DOI: 10.1039/D6QI00876C

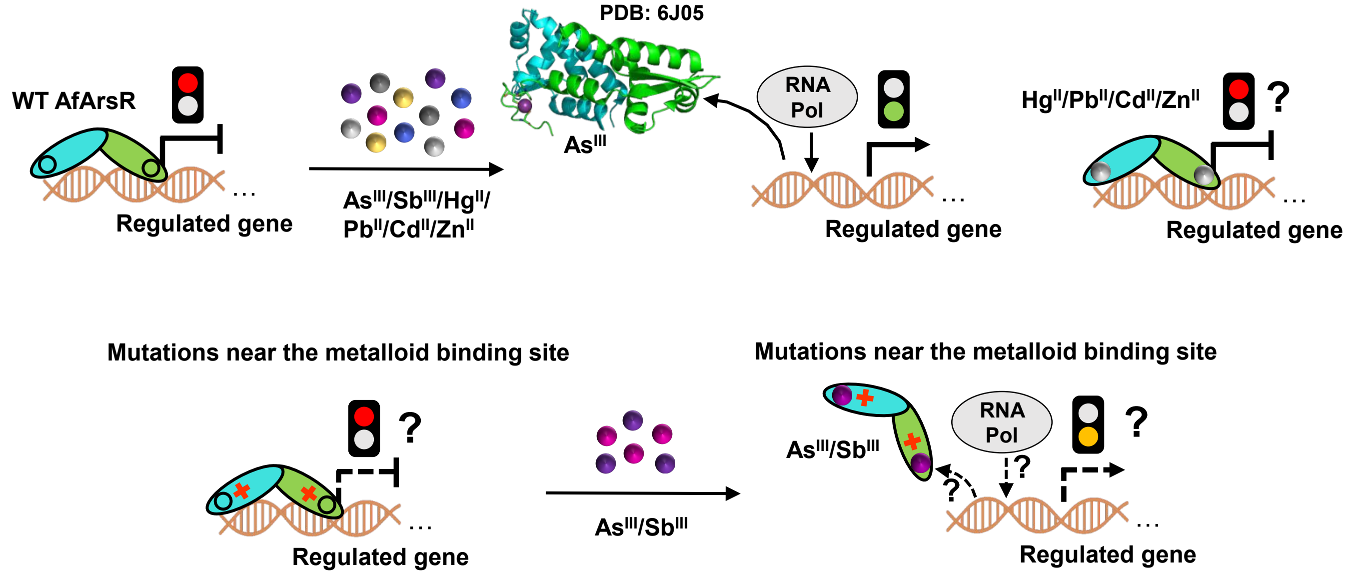

Scheme 1 Upper panels: a simplified scheme depicting the derepression mechanism of operation of the wild type AfArsR, promoted by the cognate metalloids As^{III} and Sb^{III},[9,15] and the lack of response for non-cognate thiophilic ions (a phenomenon addressed by our work). Bottom panels: the influence of single amino acid mutations in the metalloid binding domain on the repressor activity as well as the metalloid regulation efficiency of the mutant proteins. The impact of substituting the metalloid binding cysteine residues (C95, C96, C102) has already been explored[15] and the present study is targeted at studying how the exchange of other residues (R85, D101, R100, H97) near the metalloid site potentially affects metalloid recognition.

Titration by Zn^{II}, accompanied by a very weak absorbance change in the studied UV-range (presumably because the thiolate-Zn^{II} transitions occur at higher energies[42]), was terminated around a 1:1 metal ion to protein dimer ratio because of the same baseline increase phenomenon (Fig. S2C).

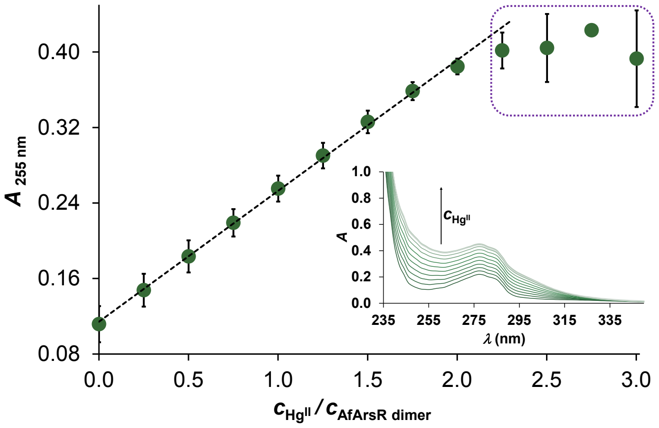

Fig. 1 Absorbances at 255 nm recorded in the titration of AfArsR by a solution of Hg^{II} at pH = 7.5 (c_{AfArsR} = 40.0 μM (for monomers) in 0.01 M phosphate buffer containing 120 μM TCEP). The symbols (averages of four independent series) and the dashed line represent the experimental data and the observed trend up to 2.0 equivalents of Hg^{II} per AfArsR dimer (data are corrected for the dilution). The dotted frame denotes points with poor reproducibility, though there was no clear indication of precipitate formation up to 3 equivalents of Hg^{II} per AfArsR$_{dim}$. The inset shows a selected series of recorded spectra, corrected for dilution.

Note that the protein bears a His-tag which may have an influence on the binding scheme of the latter two ions, though one could expect a substantially larger affinity to the Cys-rich sites, in particular regarding Cd^{II}. The recorded absorbances exhibited large scattering above 2.0 Hg^{II} equivalents per protein dimer. Although precipitation was evident only above ~3 Hg^{II} equivalents, aggregation may be suspected already from 2:1 Hg^{II}:AfArsR$_{dim}$ concentration ratio.

As^{III} and Sb^{III} binding to AfArsR also lead to a gradual absorbance change in the recorded UV-spectra and the formation of the As^{III}/Sb^{III}-bound protein complexes was demonstrated by ESI-MS, as well (Fig. S3A-B). However, the observed trends in absorbance increase follow a distinctly different pattern, as compared to the effect of the divalent metal ions (Figs. 2 and 3). We employed a model involving the dimeric protein that participates in two consecutive metalation steps, leading to the M^{III}-AfArsR$_{dim}$ and (M^{III})$_2$-AfArsR$_{dim}$ species. These steps are characterized by the following equations and the related apparent stability constants (for pH = 7.5), log$K_1^{pH7.5}$ and log$K_2^{pH7.5}$:

$$\mathrm{AfArsR_{dim} + M^{III} \rightleftharpoons M^{III}\text{-}AfArsR_{dim}} \qquad \text{(Eq. 1)}$$

$$\mathrm{M^{III}\text{-}AfArsR_{dim} + M^{III} \rightleftharpoons (M^{III})_2\text{-}AfArsR_{dim}} \qquad \text{(Eq. 2)}$$

In these equations AfArsR$_{dim}$ stands for the dimeric protein and M^{III} represents As^{III} or Sb^{III}, in their unbound form under the current conditions. The presented absorbance-change profiles indicate a rather strong binding of the first metalloid preventing unambiguous fitting of data. Thus we had to fix log$K_1^{pH7.5}$ to an estimated value (=7.0) in order to complete the fittings and obtain affinities for the binding of the second metalloids. The choice of logK_1 = 7.0 was partially based on our own data and literature data from other groups on the As^{III}-binding affinity of multiple cysteine/thiol containing ligands.

View Article Online
DOI: 10.1039/D6QI00876C

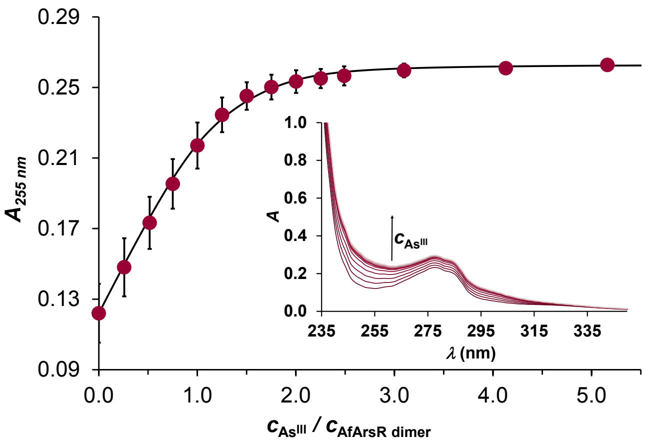

Fig. 2 Absorbances at 255 nm recorded in the titration of AfArsR by a solution of As^{III} at pH = 7.5 (c_{AfArsR} = 40.0 μM (for monomers) in 0.01 M phosphate buffer containing 120 μM TCEP). The symbols (averages of three independent series) and the solid line represent the experimental data and their fit, respectively (data are corrected for the dilution). The inset shows a selected series of the recorded spectra, corrected for dilution.

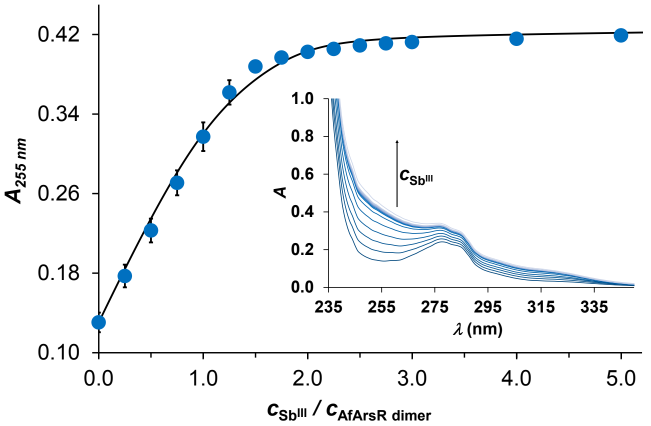

Fig. 3 Absorbances at 255 nm recorded in the titration of AfArsR by a solution of Sb^{III} at pH = 7.5 (c_{AfArsR} = 40.0 μM (for monomers) in 0.01 M phosphate buffer containing 120 μM TCEP). The symbols (averages of three independent series) and the solid line represent the experimental data and their fit, respectively (data are corrected for the dilution). The inset shows a selected series of the recorded spectra, corrected for dilution.

We have previously determined an apparent stability of log$K^{pH7.5}$ = 6.35 for the As^{III} binding of the peptidic model of AfArsR[12] and other studies with peptides displaying more separated Cys residues also indicated that the As^{III}-binding affinity to tris-thiol sites could be near log$K$ = 6.[45] Besides, the simple heavy metal ion chelator bis-thiol compound Dimercaprol (2,3-Dimercaptopropanol, BAL) is an even stronger binder of As^{III} (log$K^{pH7.0–8.1}$ = 6.6-6.9).[46,47] In a recent study Stillman and co. determined surprisingly high affinities for the consecutive binding of six As^{III} to the human metallothionein-3 protein spanning the range from log$K$ = 10.2 to 8.3 (from the first to the sixth binding event)[40] which hints that at certain protein sites metalloids may be substantially more tightly bound than it is reflected by stability data determined for model compounds.[12,41,45] The applied logK_1 = 7.0 value is also in accord with the observed linear trend in the change of absorbances up to 1:1 M^{III}:protein dimer concentration ratio, suggesting that at 1 equiv. of M^{III} per AfArsR dimer the vast majority of the added metalloid is transformed into its bound form. (Details of the model selection and the fitting procedure are explained in the ESI, see also Fig. S4 and S5.)

The stability difference for the two consecutive binding steps of both As^{III} and Sb^{III} is small but statistically significant (logK_1–logK_2 ~ 1.3 and 1.1 for As^{III} and Sb^{III}, respectively, when using the estimated logK_1 = 7.0). It is also noteworthy that the saturating segments of the absorbance trace curves, levelling off rather close to 2 equivalents of metalloids per AfArsR$_{dim}$ (Fig. 2 and 3), may be described only if the contribution of the second bound metalloid to the absorbance is remarkably weaker as compared to the effect of the first coordinated As^{III} or Sb^{III}, suggesting that the coordination environment, in particular the number of coordinated thiolates, may not be identical at the two sites. Similarly, different apparent molar absorbance values were attributed to the first and second Cd^{II}-filled sites in the homodimeric AztR.[48]

Above data indicate that metalloid binding at the two sites is not fully independent and that the coordination of the second metalloid is less favoured when the first site is loaded, i.e. there may be a negative cooperativity, which is also corroborated by EMSA studies, *vide infra*. The possibility of cooperativity in As^{III}-binding has been raised in the crystallographic study of the As^{III}-bound forms of AfArsR and CgArsR, as in contrast to CgArsR, only one of the two sites was found to be populated by As^{III} in the As^{III}-AfArsR structure.[9] In addition, Giedroc et al. demonstrated a cooperative effect in the Zn^{II} binding by another ArsR-family metalloregulator, *S. aureus* CzrA, displaying a ca. 2 orders of magnitude higher affinity for the first Zn^{II} over the second one.[49–51] Finally, there are a couple of other known examples of negative cooperativity observed for metal ion binding in other metalloregulatory proteins, too, such as the MerR family *P. putida* CadR[52] and the Fur family *B. subtilis* Zur.[33] It is also conceivable that the different affinities to the two sites are related to the asymmetry of the homodimer and differences in the structures of the two protein monomers within the dimer, as reflected also by the As^{III}-AfArsR crystal structure.[9] Asymmetry is a known structural feature in a number of homodimeric proteins, resulting in e.g. functional asymmetry in ligand binding or half-site reactivity.[53–56]

Interestingly, previous data on the As^{III}/Sb^{III}-binding of various ArsR regulators, such as those related to the *E. coli* R773 plasmid,[14] the *C. glutamicum*,[16] *C. violaceum*[17] and also the *A. ferrooxidans*[15] bacteria, obtained by different experimental techniques and often under notably different experimental conditions, indicated significantly weaker binding affinity for both metalloids (for As^{III}: K_d ~ 10– 150 μM; for Sb^{III}: K_d ~ 2–10 μM).[14,15] However, a single dissociation step, characterizing an equilibrium between the protein monomer and As^{III}/Sb^{III}, was considered in the calculation of the above cited K_d values. This can obviously lead to different constants as compared to the affinities obtained by the two-step model used in our study.

In summary, our data suggest that the binding of the two As^{III} and two Sb^{III} to the AfArsR dimer is sequential and the relative affinities for the first and second binding steps are largely

View Article Online
DOI: 10.1039/D6QI00876Q

similar for As^{III} and Sb^{III}. Titrations of the protein by divalent soft transition metal ions also indicate very efficient metalation processes with no sign of cooperativity, possibly as a consequence of the higher overall affinities. This is in line with our previous results comparing the Hg^{II} and As^{III}-coordination features of the oligopeptide model of the metalloid binding site of AfArsR, reflecting a many orders of magnitude higher affinity for Hg^{II} as compared to As^{III}.[12]

Characterization of Hg^{II} binding mode to AfArsR by ^{199m}Hg PAC spectroscopy.

The local coordination environment of the AfArsR bound Hg^{II} was also investigated by perturbed angular correlation of γ-rays (PAC) spectroscopy using the metastable ^{199m}Hg isotope (see the experimental details in the ESI).[57–59] Two short series of spectra were recorded by varying (i) the pH at a constant, substoichiometric Hg^{II}-protein concentration ratio (Fig. 4A) and (ii) the Hg^{II}-protein concentration ratio at a constant pH (pH = 7.4) (Fig. 4B). Parameters fitted to the PAC data are presented in Table S3. All the recorded spectra can be analyzed with one or two Nuclear Quadrupole Interactions (NQIs). These two NQIs are essentially the same throughout the entire dataset: NQI1 (ν_Q ≈ 1.10 GHz and η ≈ 0.7) displays a coupling constant, ν_Q, close to previous reports of trigonal planar HgS$_3$ coordination, but a significantly higher asymmetry parameter.[60–62]

Within the semi-empirical AOM applied to calculations of NQIs,[57] ideal trigonal planar HgS$_3$ and T-shaped HgS$_3$ coordination geometry[63–67] give the same coupling constant, but the axially symmetric trigonal planar structure has η = 0, while the T-shaped structure has η = 1. Thus, the observed NQI1 may reflect a HgS$_3$ structure with unusual, distorted geometry. NQI2 (ν_Q ≈ 1.50 GHz and η ≈ 0.1) exhibits high similarity to previously reported linear or distorted linear HgS$_2$ coordination.[44,60–62,68,69] High level quantum chemistry calculations indicate that the electric field gradient (EFG) changes surprisingly little upon bending HgCl$_2$,[70] so although it is likely that NQI2 reflects HgS$_2$ coordination, it may not be possible to discriminate whether the structure is linear or bent based on the ^{199m}Hg PAC data (see additional notes and the fitted parameters in Table S3).

pH series.

The change of pH in samples containing Hg^{II} and AfArsR$_{dim}$ in a 0.5:1 concentration ratio shows the gradual shift in the relative contribution of the two NQIs, *vide supra*. At pH = 9.0 the data display exclusively NQI1, i.e. a distorted HgS$_3$ structure. At pH = 7.4 the NQI1 still strongly dominates and at pH = 6.2 both species are present to a significant extent, and the relative amplitudes imply that the HgS$_2$ structure dominates, see Table S3 and Fig. 4A. Thus, the ^{199m}Hg PAC data imply that there is a pH dependent change from a mixed HgS$_2$ and HgS$_3$ coordination at low pH to pure HgS$_3$ coordination at high pH, with a tentative estimate of the pK_a around 6.4. A similar change from HgS$_2$ to HgS$_3$ coordination was observed as function of pH in other systems offering three possible coordinating thiols,[61] including the metal site model peptide of AfArsR, reflecting a very similar transformation between the two NQIs with a pK_a value falling also within the 6.0 – 7.0 range.[12] The low pH form, HgS$_2$, presumably reflects that one of the three cysteines at the metal binding site is protonated, and exhibits limited interaction with Hg^{II}. The HgS$_3$ coordination may reflect a planar structure in-between trigonal planar and T-shaped, *vide supra*, which is not unprecedented for Hg^{II} and was also proposed for the Hg^{II}-bound *E. coli* CueR protein at substoichiometric Hg^{II} concentrations,[44] as well as for the HgS$_3$-type Hg^{II} complex of the AfArsR model peptide based on PAC and EXAFS data.[12] Indeed, the fitted parameters for the HgS$_3$ species formed with the model peptide[12] and the protein are nearly the same indicating that Hg^{II} achieves a very similar coordination environment to that formed with the flexible peptide.

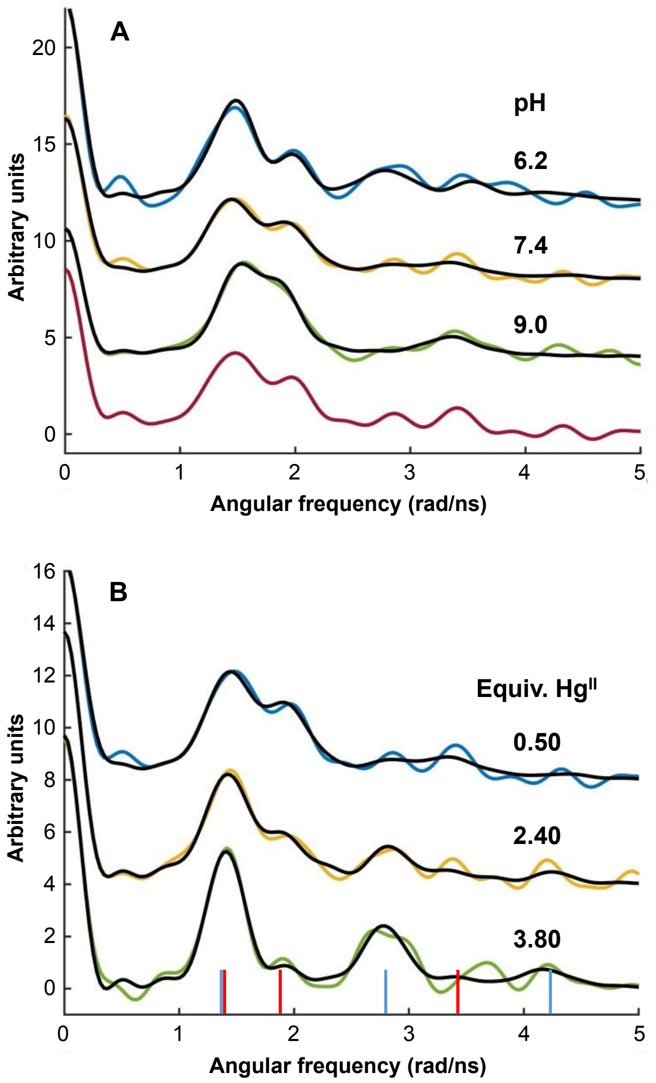

Fig. 4 A pH series (A) and Hg^{II} concentration series (B) of ^{199m}Hg PAC data for the AfArsR protein (Fourier transformed data). A) pH series was recorded at 0.5:1 Hg^{II}:protein dimer concentration ratio. B) Equiv. Hg^{II} denote molar equivalents of metal ion per protein dimer. Coloured lines represent the experimental data and black lines are the fits. The red and blue vertical lines indicate the approximate positions of the three peaks for each of the two NQIs present in the data, interpreted as (see the text) distorted HgS$_3$ (red) and HgS$_2$ (blue) structures. The bottom (purple) spectrum in panel A) is the Fourier transform of the sum of the data for the three pH values (the NQIs change slightly with pH).

View Article Online
DOI: 10.1039/D6QI00876G

Effects of changing the Hg^{II} : AfArsR dimer concentration ratio.

At low Hg^{II}-to-protein concentration ratio (= 0.50 Hg^{II} per AfArsR dimer), the ^{199m}Hg PAC signal is strongly dominated by NQI1, reflecting HgS_3 coordination, see Table S3 and Fig. 4B. Increasing the Hg^{II}:AfArsR$_{dim}$ ratio to 2.4, i.e. to more than one Hg^{II} per binding site, changes the balance between HgS_3 and HgS_2 coordination towards the latter, which can be qualitatively observed in Fig. 4B by a decrease of the intensity of the peak at 1.9 rad/ns and a concomitant increase of the intensity of the peak at 2.8 rad/ns. This most likely reflects that some of the AfArsR binding sites remain in the HgS_3 structure, while others bind more than one Hg^{II}, disrupting the HgS_3 structure and forming dinuclear Hg^{II} species with the three cysteinates, e.g. Hg_2S_3 clusters with one bridging cysteinate. A further increase of the Hg^{II}:AfArsR$_{dim}$ ratio to 3.8:1, which converts to almost two Hg^{II} equivalents per binding site, leads to essentially pure HgS_2 coordination and very little HgS_3 coordination. The almost pure HgS_2 coordination observed under such conditions may be due to Hg_2S_3 clusters at both binding sites, but the formation of Hg_3S_3 structures, with alternating S and Hg^{II} in a six-membered ring might also be a possibility. The decrease of coordination number around Hg^{II} upon increasing the Hg^{II}-to-ligand ratio was also observed for the AfArsR model peptide, reflecting an interligand Hg^{II}-bridge between two cysteine residues of two peptide molecules in a Hg_3L_2 complex. It is conceivable that a similar process occurs for the protein, leading to the precipitation described in a previous section, and indeed the PAC data display slower rotational diffusion (smaller λ, see Table S3) for the high Hg^{II} to protein ratio experiment, although the error bar is relatively large. Our findings based on the ^{199m}Hg PAC-data for the AfArsR protein are also in analogy to observations based on UV-absorption spectroscopy for a metallothionein, *M. acuminata* MT3, where the metal ion at low Hg^{II}-to-protein ratio “accepts” the HgS_4 coordination, commonly observed for Zn^{II} binding, while overloading the protein with Hg^{II} (i.e. excess Hg^{II} with respect to the 4-coordinate clusters observed with Zn^{II}), leads to the formation of HgS_2 structures.[71]

The proposed transformation from HgS_3- to HgS_2-type species of AfArsR, indicated by PAC spectroscopy, cannot be fully correlated with the UV data. The UV-titration of AfArsR by Hg^{II} (Fig. 1) does not indicate the expected change in the UV-pattern, i.e. the decrease of absorbance above ~230 nm where signature LMCT transitions for HgS_3 species tend to occur,[44,72–74] and the increase of absorbance at higher energies characteristic for the LMCT bands for HgS_2 complexes.[44,72–75] However, the variability of the measured absorbances during the UV-titration above 2 equivalents of Hg^{II} per AfArsR dimer, and the ultimate appearance of precipitate around 3:1 Hg^{II}:AfArsR$_{dim}$ concentration ratio may indicate that excess of the Hg^{II} ions leads to formation of sparingly soluble species or aggregates**.**

Effects of As^{III}, Sb^{III} and divalent metal ions on the stability of the DNA-AfArsR$_{dim}$ complex.

Electrophoretic Mobility Shift Assay (EMSA) experiments were conducted to investigate the functional selectivity of the AfArsR protein under *in vitro* conditions by comparing the effect of As^{III}, Sb^{III} and several divalent metal ions on the binding of the AfArsR dimer to a specific DNA (see the experimental details in the ESI). We also carried out EMSA by increasing the AfArsR$_{dim}$:DNA concentration ratio at a constant DNA concentration and estimated the affinity of the AfArsR dimer to the DNA using a model that involved also the dimerization equilibrium of the AfArsR monomers to the protein dimer (see Fig. S6 and other details in the ESI). The obtained log$K$ ~ 5.6 (K_d ~ 2.5 μM) for dissociation of the protein dimer from the DNA is in the same range as, but indicates a somewhat weaker affinity, than the value reported for AfArsR based on fluorescence anisotropy titrations using a fluorophore labelled DNA fragment (K_d ~ 0.9 μM).[76]

Concentration series of As^{III} and Sb^{III}, using constant AfArsR$_{dim}$ and DNA concentrations with a 6-fold protein excess (Fig. 5A) indicated the dissociation of the DNA from AfArsR at surprisingly low metalloid concentrations. As^{III} turned out to induce significant release of the DNA already at 1.0 equivalent of As^{III} per protein dimer (lane *#4* in Fig. 5A), while a notable excess of Sb^{III} was needed for the same effect (lane *#14* in Fig. 5A). On one hand, these data imply strong binding of both metalloids to the DNA-bound protein, and the concomitant release of the DNA, correlating well with the results of UV-titrations. But they also indicate some deviations from previous literature results both in terms of the observed overall affinities, and the relative effect of the two metalloids, suggesting As^{III} to be slightly better inducer. Previous DNA gel shift studies showed that in the presence of 0.1 mM As^{III}, AfArsR is completely dissociated from the 199 bp DNA, and based on fluorescence anisotropy experiments, using a much shorter fluorescein labelled DNA, Sb^{III} was found to be a more efficient inducer than As^{III}.[15] From these fluorescence anisotropy assays, K_d ~ 12 μM was estimated for the binding of a As^{III} and a ~6 times higher efficiency (lower K_d) for Sb^{III}.[15] These values reflect notably weaker affinities relative to our estimates, as well as a much larger difference between the binding strength of the two metalloids, as compared to what we propose based on UV-titrations. In addition to the difference in the applied methodologies, our model describes the As^{III}/Sb^{III} – AfArsR interaction with no DNA present, involving a two-step association/dissociation process of the metalloids from the protein dimer. In contrast to our experiments, the fluorescence anisotropy study is an indirect approach, estimating the metalloid binding affinity via monitoring the dissociation of the DNA from the protein dimer, but this process involves two interlinked equilibria, i.e. the interaction between the metalloids and the DNA-bound protein and the dissociation of the metalloid bound protein dimer from the DNA. Such differences between the applied approaches might explain the deviation between the binding constants.

It is, however, interesting that our EMSA experiments reflect a weaker efficiency of Sb^{III} in promoting the dissociation of the protein from the DNA, contrasting the rather similar AfArsR-binding profiles of As^{III} and Sb^{III} monitored by UV. We speculate that while there may not be significant differences in the affinities of As^{III} and Sb^{III} to the metalloid sites in AfArsR, the

View Article Online
DOI: 10.1039/D6QI00876C

induced conformational impacts can be different and Sb^{III} seems to destabilize less efficiently the AfArsR-DNA complex. An alternative explanation may be that while the coordination of the first As^{III} to the protein dimer is sufficient for promoting the release of the DNA from AfArsR, both binding sites need to be loaded by Sb^{III} for a comparable effect. Indeed, the possibility that a half-populated As^{III}-bound protein dimer might be a functional derepressor is in accord with the fact that the As^{III}-AfArsR crystal structure displays only one coordinating As^{III} to the protein dimer.[9] Although reactivity with partially filled metal binding sites is a known feature in several metalloenzymes displaying homodimeric or homotetrameric structures,[53] results on metalloregulatory proteins do not show a coherent picture. It was shown that both sites in the CadC homodimer has to be occupied by the inducer Cd^{II}, Pb^{II} or Zn^{II} ions to promote the dissociation of DNA from the protein,[77] and comparison of the structures of the one Zn^{II}- and two Zn^{II}-bound SmtB dimers also reflected that coordination of the second metal ion was necessary for a complete structural transition to the effective conformer.[78] As opposed to these data, coordination of the second Pb^{II} ion to the CmtR homodimer could not be observed and the single metalated form was capable of allosterically regulating DNA-binding.[79] Similarly, filling one of the two metal sites by Zn^{II} induced asymmetry in the homodimeric structure of CzrA, significantly affecting DNA binding.[49] Obviously, further studies are needed to answer these questions.

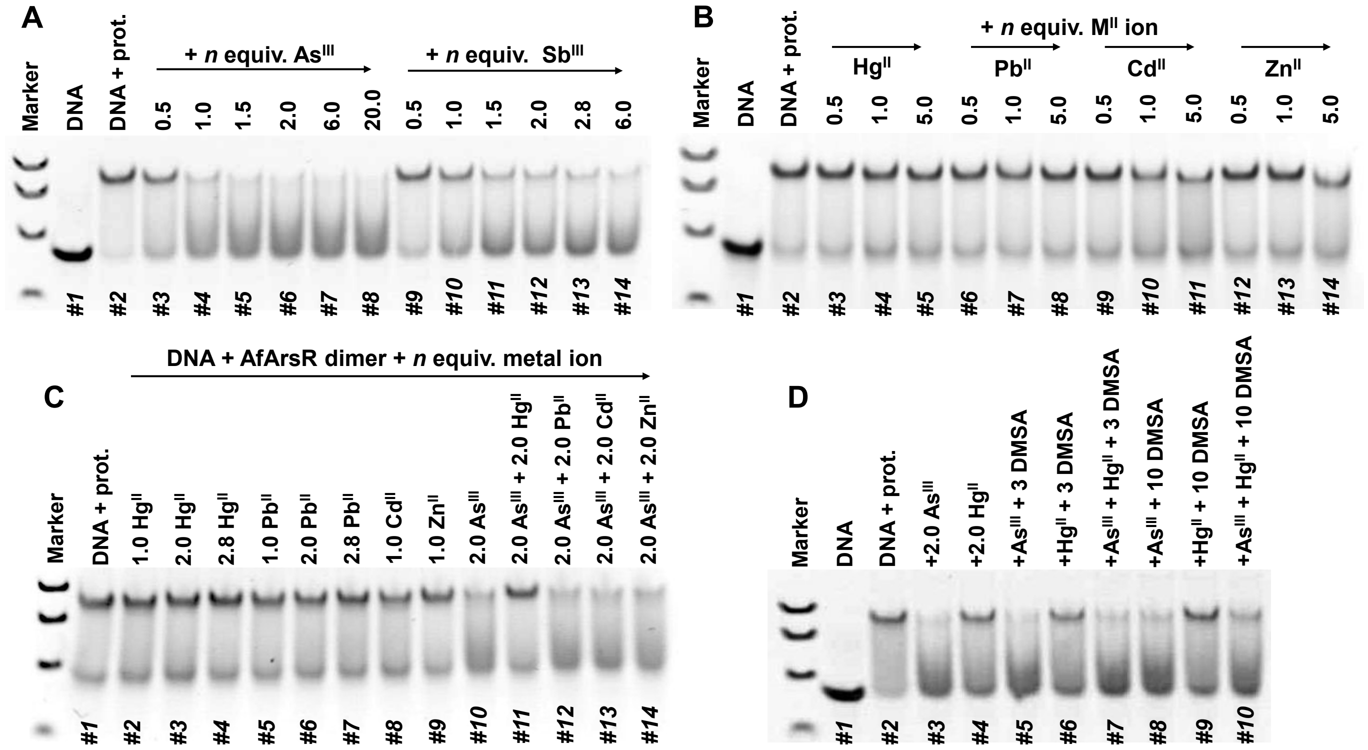

Fig. 5 Electrophoretic Mobility Shift Assays following the effect of increasing concentrations of the cognate inducers As^{III} and Sb^{III} (A), as well as the non-cognate divalent ions Hg^{II}, Pb^{II}, Cd^{II} and Zn^{II} (B) on the stability of the DNA-AfArsR$_{dim}$ complex using $c_{DNA} = 1.55\ \mu M$ and $c_{AfArsR} = 18.6\ \mu M$ (for monomers) corresponding to a 6 : 1 AfArsR dimer : DNA concentration ratio. (C) EMSA of samples containing AfArsR$_{dim}$, DNA (in a 6:1 concentration ratio) and various non-cognate metal ions in the absence and presence of As^{III}. (D) The effect of the bis-thiolate type heavy metal ion chelator dimercaptosuccinic acid (DMSA) on the DNA-AfArsR$_{dim}$ complex formation in the presence of 2.0 equivalents of As^{III} or Hg^{II} or both ($c_{DMSA} = 28\ \mu M$ and $93\ \mu M$). Equiv. of metalloids, metal ions and DMSA denote molar equivalents per protein dimer. Conditions of the EMSA experiments are described in detail in the ESI.

The effect of the divalent metal ions, Hg^{II}, Cd^{II}, Zn^{II} and Pb^{II}, on the AfArsR-DNA complex were also tested using varying M^{II}:AfArsR$_{dim}$ concentration ratios (Fig. 5B and 5C lanes *#1-9*). Remarkably, none of the samples containing comparable amounts of the protein dimer and metal ions showed significant dissociation of the DNA from the protein dimer, despite the fact that our UV-data indicated efficient binding of these divalent metal ions to AfArsR. While this is a central and so far missing observation for the inherent functional metal ion selectivity of the AfArsR protein, detected under *in vitro* conditions, it also implies that metal binding affinity is not a decisive factor in the mechanism of operation of these metalloid selective transcriptional regulators. Competition experiments were also carried out to investigate whether the effect of As^{III} on the DNA-protein complex is maintained when samples containing 2 equivalents of As^{III} per protein dimer, as well as the DNA, are incubated for 30 minutes with divalent metal ions (Fig. 5C lanes *#11-14*). Interestingly, the DNA remains dissociated from the protein after the addition of 2 equivalents of Pb^{II}, Cd^{II} or Zn^{II} (see lanes *#12-14* in Fig. 5C) but most importantly, the DNA-AfArsR$_{dim}$ complex forms again when Hg^{II} is added (lane *#11*). It reflects that the effect of As^{III} is not reversed with Pb^{II}, Cd^{II} or Zn^{II}, despite their reported strong affinities to cysteine-rich metal sites[80–83] but Hg^{II}, which is known to be bound extremely tightly to sites containing 2 or 3 Cys units,[12,73,75] fully eliminates the effect of As^{III} and allows the re-formation of the DNA-

View Article Online
DOI: 10.1039/D6QI00876C

AfArsR$_{dim}$ complex. The latter finding also indicates that the protein is shaped by the coordinated Hg^{II} into a repressor-like structure. The inefficiency of Pb^{II}, Cd^{II} or Zn^{II} to interfere with the As^{III} response by the protein might be of kinetic origins (slow dissociation of As^{III}), but the observed effect of the added Hg^{II} appears to be in conflict with this interpretation. However, Hg^{II} displays a preference for linear bisthiolato-coordination, and might coordinate to two of the thiolates forming a (distorted) linear structure, perturbing the binding site to an extent that it eliminates the effect of As^{III}, even if As^{III} would remain bound. The other metal ions usually require higher coordination numbers, and are more promiscuous in terms of coordination geometries, and might therefore not have this effect. In conclusion, the most interesting facet of these results is the diminished functional selectivity of the protein for As^{III} in the presence of Hg^{II} under *in vitro* conditions, and this is elaborated further in the following section.

Effect of As^{III}, Sb^{III} and divalent metal ions on the stability of the DNA-AfArsR$_{dim}$ complex studied by the I-Block assay *in vivo* in the bacterial cells.

The development of biosensor/bioreporter constructs for arsenic has been a focus of bioanalytical research for many years. Several whole-cell based approaches have been utilized, such as those based on the regulation of the *luciferase* gene, the *lacZ* gene (gene of β-galactosidase) or the *(e)gfp* gene as reporter elements.[84] In this study, the purpose of using a recently developed and further optimized bioreporter system, the I-Block assay,[39,85] was to compare the results of *in vitro* EMSA experiments with the intracellular influence of As^{III}, Sb^{III}, as well as Hg^{II}, Cd^{II}, Zn^{II} and Pb^{II} on the stability of the DNA-AfArsR$_{dim}$ complex. This assay is based on the detection of β-galactosidase activity, resulting in a colour reaction in the modified *E. coli* cells, when the dimeric AfArsR protein is bound to its target DNA sequence. On the other hand, the expression of β-galactosidase enzyme is prevented by the LacI inhibitory protein that is expressed in these cells if AfArsR dissociates from the target DNA, e.g. as a consequence of the coordination of the inducers to the metalation sites. The production of the bioreporter and control DNA constructs, details of their operation, as well as the conditions of the I-Block experiments executed either with pre-incubated cells in test tubes or with bacterial cultures grown on Luria agar plates, the statistical analysis of the obtained results and supplementary discussion with figures in addition to those presented in the article below, are all found in the ESI.

Fig. 6 displays the relative inhibitory effect of the studied metalloids and metal ions on the β-galactosidase activity (reflecting the ability of these to disrupt the DNA-AfArsR$_{dim}$ complex), as compared to cells grown in a metalloid/metal ion free nutrient broth and to the control system expressing LacI but not AfArsR. (A detailed concentration profiles for As^{III} and Sb^{III} are presented in Fig. S9.) Images of Luria agar plates with bacterial cultures grown in media in the absence and presence of metalloids/metal ions carry a similar information (Fig. S8). Note, that in comparison to *in vitro* studies, the operation of a bioreporter is affected by much more, laboriously controllable factors, such as the uptake of the metal ions and their transport inside the cells, as well as the distribution and binding of the metal ions to other possible intracellular binders, i.e. the available metal pool inside the cells after incubation using a certain metal ion concentration, etc..

Nonetheless, the presented relative induction values are in accord with the expected response for the added metalloids, and reflect no significant response for the divalent metal ions, in correlation with the *in vitro* observations. Similar to the EMSA experiments, the metalloids display functional selectivity by allowing the binding of As^{III} and Sb^{III} and thereby the inhibition of β-galactosidase enzyme (i.e. promoting the expression of LacI) even in the presence of identical concentration of the non-cognate Cd^{II}, Zn^{II}, Pb^{II} and Hg^{II} ions. Thus, the only difference between the two assays is seen in the system where As^{III} and Hg^{II} are combined. This suggests that despite the presumably enormous difference between the affinities of Hg^{II} and As^{III} to the effector binding sites of AfArsR,[12] Hg^{II}-binding to the protein is rather unlikely because of the very limited available Hg^{II}-pool, as a consequence of the competitive effect of a number of cellular thiol containing molecules, such as Cys-rich proteins, glutathione, etc. (though other intracellular factors, such as pH or ionic strength, may also affect the *in vivo* findings).

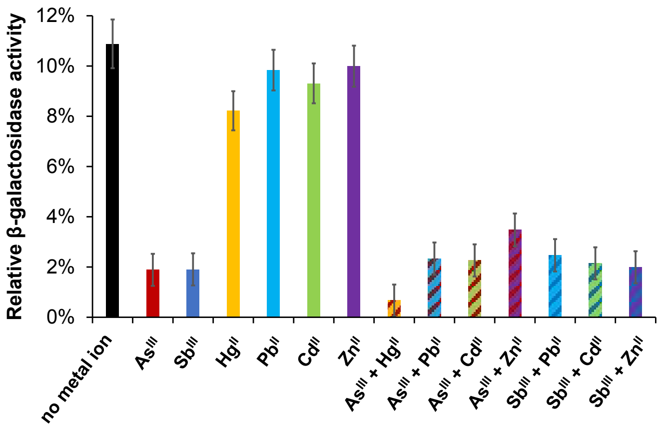

Fig. 6 Variation of the relative β-galactosidase activities (given in relative Miller units) measured in I-Block assays for an AfArsR bioreporter construct in the presence of metalloids and metal ions added to the nutrient broth in identical concentration (20 μM). The right side of the chart presents "competition" experiments for As^{III} or Sb^{III} combined with a divalent metal ion, both used in 20 μM concentration. The presented data are averages of 4-12 independent experiments (varied between systems). Experimental details of the I-Block assays and statistical analysis of the data, indicating the significance of activity changes at a $p = 0.05$ confidence level (Table S4), are found in the ESI.

To test this assumption, we carried out an additional EMSA assay, *vide supra*, where the effect of As^{III} and Hg^{II} on the DNA-AfArsR$_{dim}$ complex was compared in the presence and absence of dimercaptosuccinic acid (DMSA), a well-known and clinically recommended chelator of Hg^{II} [86,87] that also possess a notable affinity for As^{III} [88,89] (Fig. 5D). These competition type EMSA experiments showed that Hg^{II} is not able to restore the DNA-AfArsR$_{dim}$ complex in the presence of the inducer As^{III} and 3 equivalents of DMSA (lane *#7* in Fig. 5D), due to the high stability of the Hg^{II}-DMSA complexes[86,87] (note the large discrepancies in the published stabilities of Hg^{II} complexes formed with bis-thiol

View Article Online
DOI: 10.1039/D6QI00876G

type chelators, especially, DMSA).[86,87,90,91] Based on this observation, even a small excess of DMSA over Hg^{II} protects the protein from the competing Hg^{II} ions. Small excess of DMSA, relative to concentration of As^{III}, does not attenuate the effect of the metalloid on the DNA-AfArsR$_{dim}$ complex (see lanes *#3* and *#5* in Fig. 5D), most likely because of the notably weaker As^{III}-binding affinity of DMSA[88,89] as compared to the binding strength of As^{III} at the AfArsR binding sites. However, one may notice that the band of the DNA-protein complex becomes slightly stronger when DMSA is used in a 10-fold excess over As^{III}, independently of the presence of Hg^{II} (lanes *#8* and *#10* in Fig. 5D), indicating that DMSA, at higher concentrations, may start withdrawing a fraction of As^{III} from the protein.

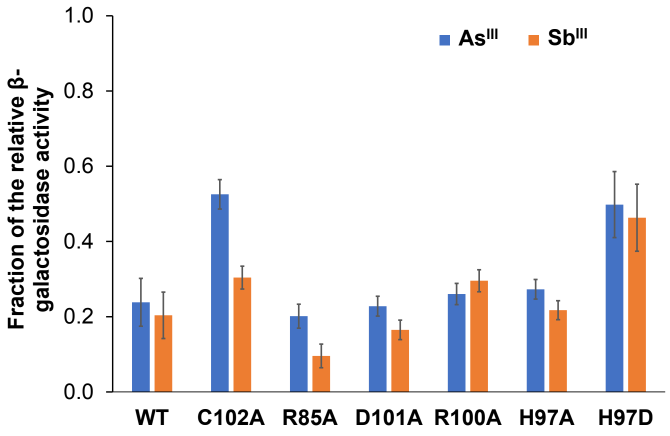

Fig. 7 Fraction of the relative β-galactosidase activities, showing ratios of the activity values measured for the bioreporter constructs of the different AfArsR variants in the absence and presence of metalloids added to the nutrient broth in a concentration of 20 μM. The presented data are averages of 4-12 independent experiments (varied between systems). Experimental details of the I-Block assays and statistical analysis, indicating the significance of the deviations as compared to the data measured for the WT system at a $p = 0.05$ confidence level (Table S5 and S6), are found in the ESI.

Several mutants of AfArsR were established within the I-Block bioreporter DNA constructs to gain further insight into the mechanism of metalloid recognition at the molecular level, in terms of the role/importance of selected amino acids. The potential structural roles of the mutated amino acids are depicted in the ESI in Fig. S12. In addition to single and double mutations at the metalloid binding Cys residues (C95A, C96A, C102A, C95A/C96A), the positively charged R100 and the negatively charged D101 amino acids were replaced for the neutral alanines in separate constructs (R100A, D101A) to explore whether these charged residues, in the proximity of the metalloid binding sites, play a role in the recognition event. As Fig. S13 demonstrates, mutations of C95 or C96, but especially the former, completely blocks the β-galactosidase activity, that is, the interaction between the DNA and the protein is disrupted. This is in line with previous data about the role of these residues indicating that they are not only essential for accepting the metalloids, but are also important for the binding of the apo protein to the DNA.[15] Indeed, metalloid coordination to these residues may interfere with or prevent this function of the C95/C96 residues, hence the protein dissociates from the DNA. Rosen et al. also proposed that C102 is not as crucial for the binding of As^{III}, but it is needed for forming a high(er) affinity site.[15] Our data indicate, that the C102S mutant is, indeed, a functional repressor protein that responds both to As^{III} and Sb^{III}, but the inhibition of the β-galactosidase activity was found to be somewhat less effective compared to the wild type AfArsR (Fig. 7, Fig. S13 and Table S6), and this is also in accord with reported data.[15]

The impact of three further mutations in the protein were tested for the functionality of the repressor and its responsiveness to the inducers. A closer look at the metalloid site in the crystal structure of the As^{III}-bound AfArsR[9] highlights possible weak interactions between R85 from the $\alpha5$ dimerization helix and the A105 carbonyl within the metalloid binding segment. The introduced R85A mutation resulted in a perfectly functional repressor showing the same efficient response to As^{III} and Sb^{III} as the WT protein (Fig. 7 and Fig. S13), suggesting no specific role of the R85 arginine in the metalloid recognition event. Finally, the H97 residue within the metalloid binding segment was replaced first by Ala (H97A) and then by the negatively charged Asp unit (H97D). Based on the crystal structures of As^{III}-AfArsR[9] and As^{III}-CgArsR[9] and our DFT optimized small models of the As^{III}- and Hg^{II}-bound structures of the metal site, we hypothesized that the amide NH between C96 and H97 might form a H-bond with the last carbonyl oxygen of the $\alpha2$ helix,[12] or else, a potentially protonated sidechain imidazole may also form a link towards the negatively charged end of the helix dipole. With the latter mutations we aimed to test whether such interactions are realistic and could be part of the signalling pathway from the metal site to the DNA binding domain.[92] The H97A mutation has no noticeable effect on the functionality of the protein and accordingly, participation of the sidechain imidazole group of the H97 histidine in metalloid recognition is unlikely. However, the H97D mutant, carrying a negatively charged aspartate, displays a notably weaker sensitivity in responding to the metalloids (Fig. 7, Table S6). This receives a further support from *in vitro* EMSA experiments, carried out in samples of the purified H97D AfArsR mutant (see the ESI), following the As^{III} promoted release of the H97D AfArsR from the DNA (Fig. S7). As reflected by the data, the complete dissociation of the mutant requires a slightly larger As^{III} excess (2.0-6.0-fold) over the H97D AfArsR dimer than that needed for the dissociation of the WT protein (Fig. 5A). While the various data collected for the wild type, the H97A and H97D variants, do not allow suggesting a specific mechanism for the signaling event, but they indicate that modifications at position 97 may affect the efficiency of the protein in responding to As^{III} and Sb^{III} and ultimately influence the metalloid recognition process.

Conclusions

Binding of the inducer As^{III}, Sb^{III} and the non-cognate ions Hg^{II}, Pb^{II}, Cd^{II} and Zn^{II} to the AfArsR protein, as well as their influence on the release of the regulated operator DNA from the protein-DNA complex were investigated with an aim to explore selectivity in metalloid sensing. Data from UV-titration experiments point to a sequential As^{III} and Sb^{III} binding scheme at the two effector binding sites in the homodimer and possibly differences in the coordination environment of the two bound metalloids.

The divalent metal ions were shown to bind very efficiently to AfArsR, providing support for our previous argument that the metalloid selectivity of these regulators is not an affinity-based feature.[12] The propensity of As^{III} and Sb^{III} to weaken the binding between AfArsR and the regulated specific DNA was monitored by Electrophoretic Mobility Shift Assays, suggesting As^{III} to be the more efficient inducer. Indeed, the nearly complete release of DNA was observed at As^{III} concentrations corresponding to one As^{III} equivalent per $AfArsR_{dim}$, indicating that even a half As^{III}-loaded protein dimer may be a functional complex. Whether the binding of only one As^{III} to $AfArsR_{dim}$ also induces a structural switch to a derepressor form, as implied by our EMSA data, needs a further elucidation.

As a clear *in vitro* indication of the intrinsic functional selectivity of AfArsR, allowing the protein to discriminate between cognate and non-cognate ions, EMSA experiments were carried out with the various divalent metal ions, demonstrating only minor dissociation of the DNA-$AfArsR_{dim}$ complex, clearly contrasting the effect of the metalloids. In competition EMSA measurements, Hg^{II} was the only ion that could prevent As^{III} from inducing the release of DNA from the protein. However, similar inhibitory action of Hg^{II} was not observed inside bacterial cells via a bioreporter assay, nor upon addition of the heavy metal chelator DMSA in a repeated EMSA experiment, indicating that inhibition by Hg^{II} may not be significant within the cells.

Intracellular bioreporter constructs, based on the I-Block system utilizing AfArsR as the sensory element, responded only to As^{III} and Sb^{III} and remained “silent” for the studied divalent metal ions. Selected mutations were introduced in the *arsR* gene to tune the metalloid response of the bioreporter constructs, potentially alluding to roles of the replaced amino acid residues of AfArsR in the metalloid selection/derepression event. We confirmed the essential roles of Cys95 and Cys96 and the assistance of C102 in the protein function, but also showed that the His97Asp mutation affects both DNA binding and the metalloid response of the protein.

Author contributions

A.J. coordinated the whole project. A.J. and Gy.B. made the conceptualization of the experiments. A.T. A.J., Gy.B. and L.H. co-wrote the manuscript. A.T. and A.J. performed the analysis of equilibrium data. A.T., B.H., R.S.Gy. and Z.H.N. carried out the production and purification of the wild type and H97D mutant proteins, including the production of mutants in bioreporter constructs. K.K, A.K., A.T. and H.B. designed and executed all the bioreporter-based experiments, including data analysis and presentation. R.S.Gy. carried out I-Block experiments on Luria agar plates and the experiments with the H97D mutant AfArsR. A.T. and Z.H.N. directed and analysed the EMSA assays. É.H.-G. conducted ESI-MS experiments with data analysis and presentation. J.G.C. and J.S. organized the PAC studies including the managing of the physics and chemistry preparation labs, the beamline and the instrumental setups. A.T. and A.J. prepared the samples for PAC, J.S. and T.T.D. carried out the experiments, run the setups and collected the data, analysed afterwards by L.H.

Conflicts of interest

There are no conflicts to declare.

Data availability

The data supporting this article have been included as part of the Supplementary Information (ESI). Procedures of protein production including purification protocols, details of sample preparations, experimental methods and data fitting as well as figures and tables presenting spectral data and electrophoretic gel mobility shift assays are made available in the ESI. The code for PSEQUAD can be found at https://www.staff.u-szeged.hu/~peintler/enprogs.htm#psequad. The version of the code employed for this study is version 5.31.

Acknowledgements

This work was supported by the Hungarian National Research, Development and Innovation Office (NKFIH) within ADVANCED_24 projects, grant No. 150330 and MEC_R 149738 and by the Hungarian Academy of Sciences and Japan Society for the Promotion of Science (JSPS NKM2024-15/2024). We thank the financial support provided by the Federal Ministry of Research, Technology and Space (BMFTR) through Grants No. 05K22PGA, 05K25PGA and 05K22PGB, alongside support from the ISOLDE collaboration. We acknowledge the support of the European Union’s Horizon Europe Framework research and innovation programme under grant agreement no. 101057511 (EURO-LABS) and of the European Union’s Horizon 2020 Framework research and innovation program under grant agreement no. 654002 (ENSAR2). Support from FCT-Portugal, projects UIDP/04349/2020 and 2024.00223.CERN funded by the PRR, RE-C06-i06.m02, through EMRP and FCT (https://doi.org/10.54499/2024.00223.CERN) is also acknowledged. The gene of the AfArsR protein, inserted in a pBAD vector, was kindly provided by Prof. Saravanamuthu Thiyagarajan (Institute of Bioinformatics and Applied Biotechnology, Bengaluru, India) and we are really grateful for his invaluable help. The authors also thank Adeleh Mokhles Gerami (CERN) for her assistance in recording the ^{199m}Hg PAC data.

Notes and references

1 L. S. Busenlehner, M. A. Pennella, D. P. Giedroc, The SmtB/ArsR family of metalloregulatory transcriptional repressors: structural insights into prokaryotic metal resistance, *FEMS Microbiol. Rev.*, 2003, **27**, 131–143.
2 C. Xu, T. Zhou, M. Kuroda, B. P. Rosen, Metalloid resistance mechanisms in prokaryotes, *J. Biochem.*, 1998, **123**, 16–23.
3 B. P. Rosen, Biochemistry of arsenic detoxification, *FEBS Lett.*, 2002, **529**, 86–92.
4 M. A. Pennella, J. E. Shokes, N. J. Cosper, R. A. Scott, D. P. Giedroc, Structural elements of metal selectivity in metal

sensor proteins, *Proc. Natl. Acad. Sci. USA*, 2003, **100**, 3713–3718.

5 S. R. Kar, A. C. Adams, J. Lebowitz, K. B. Taylor, L. M. Hall, The cyanobacterial repressor SmtB is predominantly a dimer and binds two Zn^{2+} ions per subunit, *Biochemistry*, 1997, **36**, 15343–15348.

6 M. Semavina, D. Beckett, T. M. Logan, Metal-linked dimerization in the iron-dependent regulator from *Mycobacterium tuberculosis*, *Biochemistry*, 2006, **45**, 12480–12490.

7 L. S. Busenlehner, N. J. Cosper, R. A. Scott, B. P. Rosen, M. D. Wong, D. P. Giedroc, Spectroscopic properties of the metalloregulatory Cd(II) and Pb(II) sites of *S. aureus* pI258 CadC, *Biochemistry*, 2001, **40**, 4426–4436.

8 C. Xu, B. P. Rosen, Dimerization is essential for DNA binding and repression by the ArsR metalloregulatory protein of *Escherichia coli*, *J. Biol. Chem.*, 1997, **272**, 15734–15738.

9 C. Prabaharan, P. Kandavelu, C. Packianathan, B. P. Rosen, S. Thiyagarajan, Structures of two ArsR As(III)-responsive transcriptional repressors: Implications for the mechanism of derepression, *J. Struct. Biol*., 2019, **207**, 209–217.

10 J. Chen, V. S. Nadar, B. P. Rosen, A novel MAs(III)-selective ArsR transcriptional repressor, *Mol. Microbiol.*, 2017, **106**, 469–478.

11 Y. Zhang, W. Wu, K. Huang, F.-J. Zhao, A new type of ArsR transcriptional repressor controls transcription of the arsenic resistance operon of *Arsenicibacter rosenii* SM-1, *mLife*, 2025, **4**, 96–100.

12 A. Tóth, K. Sajdik, B. Gyurcsik, Z.H. Nafaee, E. Wéber, Z. Kele, N. J. Christensen, J. Schell, J. G. Correia, K. G. V. Sigfridsson Clauss, R. K. Pittkowski, P. W. Thulstrup, L. Hemmingsen, A. Jancsó, As^{III} selectively induces a disorder-to-order transition in the metalloid binding region of the AfArsR protein, *J. Am. Chem. Soc.*, 2024, **146**, 17009–17022.

13 J. Wu, B. P. Rosen, Metalloregulated expression of the *ars* operon, *J. Biol. Chem.*, 1993, **268**, 52–58.

14 W. Shi, J. Dong, R. A. Scott, M. Y. Ksenzenko, B. P. Rosen, The role of arsenic-thiol interactions in metalloregulation of the *ars* operon, *J. Biol. Chem*., 1996, **271**, 9291–9297.

15 J. Qin, H.-L. Fu, J. Ye, K. Z. Bencze, T. L. Stemmler, D. E. Rawlings, B. P. Rosen, Convergent evolution of a new arsenic binding site in the ArsR/SmtB family of metalloregulators, *J. Biol. Chem*., 2007, **282**, 34346–34355.

16 E. Ordonez, S. Thiyagarajan, J. D. Cook, T. L. Stemmler, J. A. Gil, L. M. Mateos, B. P. Rosen, Evolution of metal(loid) binding sites in transcriptional regulators, *J. Biol. Chem*., 2008, **283**, 25706–25714.

17 L. M. Arruda, L. M. O. Monteiro, R. Silva-Rocha, The *Chromobacterium violaceum* ArsR arsenite repressor exerts tighter control on its cognate promoter than the *Escherichia coli* system, *Front. Microbiol*., 2016, **7**, 1851.

18 V. H.-C. Liao, K.-L. Ou, Development and testing of a green fluorescent protein-based bacterial biosensor for measuring bioavailable arsenic in contaminated groundwater samples, *Environ. Toxicol. Chem.*, 2005, **24**, 1624–1631.

19 W. Lee, H. Kim, G. Jang, B.-G. Kim, Y. Yoon, Antimony sensing whole-cell bioreporters derived from ArsR genetic engineering, *Appl. Microbiol. Biotechnol.*, 2020, **104**, 2691–2699.

20 E. Elcin, H. A. Öktem, Immobilization of fluorescent bacterial bioreporter for arsenic detection, *J. Environ. Health Sci. Eng.*, 2020, **18**, 137–148.

21 J. Stocker, D. Balluch, M. Gsell, H. Harms, J. Feliciano, S. Daunert, K. A. Malik, J. R. van der Meer, Development of a set of simple bacterial biosensors for quantitative and rapid measurements of arsenite and arsenate in potable water, *Environ. Sci. Technol.,* 2003, **37,** 4743–4750.

22 L. A. Pola-Lopez, J. L. Camas-Anzueto, A. Martinez-Antonio, M. C. Lujan-Hidalgo, G. Anzueto-Sanchez, V. M. Ruiz-Valdiviezo, R. Grajales-Coutino, Novel arsenic biosensor “POLA” obtained by a genetically modified *E. coli* bioreporter cell, *Sensors Actuat, B Chem.,* 2017, **254,** 1061–1068.

23 P. Li, Y. Wang, X. Yuan, X. Liu, C. Liu, X. Fu, D. Sun, Y. Dang, D. E. Holmes, Development of a whole-cell biosensor based on an ArsR-P_{ars} regulatory circuit from *Geobacter sulfurreducens*, *Environ. Sci. Ecotechnol.,* 2021, **6,** 100092.

24 Q. Hu, L. Li, Y. Wang, W. Zhao, H. Qi, G. Zhuang, Construction of WCB-11: A novel *phi*YFP arsenic-resistant whole-cell biosensor, *J. Environ. Sci.,* 2010, **22**, 1469–1474.

25 X. Jia, R. Bu, T. Zhao, K. Wu, Sensitive and specific whole-cell biosensor for arsenic detection, *Appl. Environ. Microbiol.,* 2019, **85,** e00694-19.

26 S. Ramanathan, W. Shi, B. P. Rosen, S. Daunert, Sensing antimonite and arsenite at the subattomole level with genetically engineered bioluminescent bacteria, *Anal. Chem.,* 1997, **69,** 3380–3384.

27 D. L. Scott, S. Ramanathan, W. Shi, B. P. Rosen, S. Daunert, Genetically engineered bacteria: Electrochemical sensing systems for antimonite and arsenite, *Anal. Chem.,* 1997, **69,** 16–20.

28 F. Cortés-Salazar, S. Beggah, J. R. van der Meer, H. H. Girault, Electrochemical As(III) whole-cell based biochip sensor, *Biosens. Bioelectron.,* 2013, **47,** 237–242.

29 N. Soleja, O. Manzoor, P. Khan, M. Mohsin, Engineering genetically encoded FRET-based nanosensors for real time display of arsenic (As^{3+}) dynamics in living cells, *Sci. Rep.,* 2019, **9,** 11240.

30 S. S. Khan, Y. Shen, M. Q. Fatmi, R. E. Campbell, H. Bokhari, Design and prototyping of genetically encoded arsenic biosensors based on transcriptional regulator AfArsR, *Biomolecules,* 2021, **11**, 1276.

31 K. Turner, S. Joel, J. Feliciano, A. Feltus, P. Pasini, D. Wynn, P. Dau, E. Dikici, S. K. Deo, S. Daunert, Transcriptional regulatory proteins as biosensing tools, *Chem. Commun.*, 2017, **53**, 6820–6823.

32 B. Wang, M. Barahona, M. Buck, *Nucleic Acids Res.,* Engineering modular and tunable genetic amplifiers for scaling transcriptional signals in cascaded gene networks, 2014, **42,** 9484–9492.

33 Z. Ma, S. E. Gabriel, J. D. Helmann, Sequential binding and sensing of Zn(II) by *Bacillus subtilis* Zur, *Nucleic Acids Res.* 2011, **39**, 9130–9138.

34 M. D. Wong, Y.-F Lin, B. P. Rosen, The Soft Metal Ion Binding Sites in the *Staphylococcus aureus* pI258 CadC Cd(II)/Pb(II)/Zn(II)-responsive Repressor Are Formed between Subunits of the Homodimer, *J. Biol. Chem.*, 2002, **43**, 40930–40936.

35 L. M. Utschig, J. G. Wright, T. V. O'Halloran, Biochemical and Spectroscopic Probes of Mercury(II) Coordination Environments in Proteins, *Methods in Enzymol.*, 1993, **226**, 71–97.

36 D. Wang, S. Huang, P. Liu, X. Liu, Y. He, W. Chen, Q. Hu, T. Wei, J. Gan, J. Ma, H. Chen, Structural Analysis of the Hg(II)-Regulatory Protein Tn501 MerR from Pseudomonas aeruginosa, *Sci. Rep.*, 2016, **6**, 33391.

37 G. Zampella, K. P. Neupane, L. De Gioia, V. L. Pecoraro, The Importance of Stereochemically Active Lone Pairs For Influencing Pb^{II} and As^{III} Protein Binding, *Chem. Eur. J.*, 2012, **18**, 2040–2050.

38 C.-Ye Hui, Y. Guo, X.-Q. Yang, W. Zhang, X.-Q. Huang, Surface display of metal binding domain derived from PbrR on Escherichia coli specifically increases lead(II) adsorption, *Biotechnol. Lett.*, 2018, **40**, 837–845.

39 S. Szentes, N. Zsibrita, M. Koncz, E. Zsigmond, P. Salamon, Z. Pletl, A. Kiss, I-Block: a simple *Escherichia coli*-based assay for

View Article Online
DOI: 10.1039/D6QI00876C

studying sequence-specific DNA binding of proteins, *Nucleic Acids Res.*, 2020, **48**, e28.

40 A. T. Yuan, M. J. Stillman, Arsenic binding to human metallothionein-3, *Chem. Sci.*, 2023, **14**, 5756–5767.

41 L. I. Szekeres, P. Maldivi, C. Lebrun, C. Gateau, E. Mesterhazy, P. Delangle, A. Jancso, Tristhiolato pseudopeptides bind arsenic(III) in an AsS_3 coordination environment imitating metalloid binding sites in proteins, *Inorg. Chem.*, 2023, **62**, 6817–6824.

42 M. Vasak, J. H. R. Kaegi, H. Allen, O. Hill, Zinc(II), cadmium(II), and mercury(II) thiolate transitions in metallothionein, *Biochemistry*, 1981, **20**, 2852–2856.

43 M. Łuczkowski, M. Stachura, V. Schirf, B. Demeler, L. Hemmingsen, V. L. Pecoraro, Design of thiolate rich metal binding sites within a peptidic framework, *Inorg. Chem*., 2008, **47**, 10875–10888.

44 R. K. Balogh, B. Gyurcsik, É. Hunyadi-Gulyás, J. Schell, P. W. Thulstrup, L. Hemmingsen, A. Jancsó, C-terminal cysteines of CueR act as auxiliary metal site ligands upon Hg^{II} binding—A mechanism to prevent transcriptional activation by divalent metal ions? *Chem. Eur. J*., 2019, **25**, 15030–15035.

45 K. T. Kitchin, K. Wallace, Arsenite binding to synthetic peptides based on the Zn finger region and the estrogen binding region of the human estrogen receptor-α, *Toxicol. Appl. Pharmacol*., 2005, **206**, 66–72.

46 W. L. Zahler, W. W Cleland, A specific and sensitive assay for disulfides, *J. Biol. Chem*., 1968, **243**, 716–719.

47 L. I. Szekeres, B. Gyurcsik, T. Kiss, Z. Kele, A. Jancsó, Interaction of arsenous acid with the dithiol-type chelator British anti-Lewisite (BAL): Structure and stability of species formed in an unexpectedly complex system, *Inorg. Chem*., 2018, **57**, 7191–7200.

48 T. Liu, J. W. Golden, D. P. Giedroc, A zinc(II)/lead(II)/cadmium(II)-inducible operon from the cyanobacterium *Anabaena* is regulated by AztR, an α3N ArsR/SmtB metalloregulator, *Biochemistry*, 2005, **44**, 8673–8683.

49 S. Lee, A. I. Arunkumar, X. Chen, D. P. Giedroc, Structural insights into homo- and heterotropic allosteric coupling in the zinc sensor *S. aureus* CzrA from covalently fused dimers, *J. Am. Chem. Soc.*, 2006, **128**, 1937–1947.

50 N. E. Grossoehme, D. P. Giedroc, Energetics of allosteric negative coupling in the zinc sensor *S. aureus* CzrA, *J. Am. Chem. Soc.*, 2009, **131**, 17860–17870.

51 H. Reyes-Caballero, G. C. Campanello, D. P. Giedroc, Metalloregulatory proteins: Metal selectivity and allosteric switching, *Biophys. Chem.*, 2011, **156**, 103–114.

52 X. Liu, Q. Hu, J. Yang, S. Huang, T. Wei, W. Chen, Y. He, D. Wang, Z. Liu, K. Wang, J. Gan, H. Chen, Selective cadmium regulation mediated by a cooperative binding mechanism in CadR, *Proc. Natl. Acad. Sci. USA*, 2019, **116**, 20398–20403.

53 R. C. Nguyen, C. Stagliano, A. Liu, Structural insights into the half-of-sites reactivity in homodimeric and homotetrameric metalloenzymes, *Curr. Opin. Chem. Biol.*, 2023, **75**, 102332.

54 L. S. Swapna, K. Srikeerthana N. Srinivasan, Extent of Structural Asymmetry in Homodimeric Proteins: Prevalence and Relevance, *PLoS One,* 2012, **7**, e36688.

55 J. H. Brown, Breaking symmetry in protein dimers: Designs and functions, *Prot. Sci.,* 2006, **15**, 1–13.

56 Z. Ye, P. G. Needham, S. K. Estabrooks, S. K. Whitaker, B. L. Garcia, S. Misra, J. L. Brodsky, C. J. Camacho, **Symmetry** breaking during homodimeric assembly activates an E3 ubiquitin ligase, *Sci. Rep.*, 2017, **7**, 1789.

57 L. Hemmingsen, K. N. Sas, E. Danielsen, Biological applications of perturbed angular correlations of γ-ray spectroscopy, *Chem. Rev.*, 2004, **104**, 4027–4061.

58 L. Hemmingsen, M. Stachura P. W. Thulstrup, N. J. Christensen, K. Johnston, Selected applications of perturbed angular correlation of γ-rays (PAC) spectroscopy in biochemistry, *Hyperfine Interact.*, 2010, **197**, 255–267.

59 A. Jancso, J. G. Correia, A. Gottberg, J. Schell, M. Stachura, D. Szunyogh, S. Pallada, D. C. Lupascu, M. Kowalska, L. Hemmingsen, TDPAC and β-NMR applications in chemistry and biochemistry, *J. Phys. G Nucl. Part. Phys.*, 2017, **44**, 064003.

60 W. Tröger, Nuclear probes in life sciences, *Hyperfine Interact.*, 1999, **120/121**, 117–128.

61 O. Iranzo, P. W. Thulstrup, S.-b. Ryu, L. Hemmingsen, V. L. Pecoraro, The application of ^{199}Hg NMR and ^{199m}Hg perturbed angular correlation (PAC) spectroscopy to define the biological chemistry of Hg^{II}: A case study with designed two- and three-stranded coiled coils, *Chem. Eur. J.*, 2007, **13**, 9178–9190.

62 R. K. Balogh, A. Jancso, B. Gyurcsik, J. Schell, J. G. Correia, P. W. Thulstrup, L. Hemmingsen, S77C-ΔC7-CueR: a ^{199m}Hg PAC study of the protein metal site structure, *Hyperfine Interact.*, 2024, **245**, 43.

63 A. Manceau, K. L. Nagy, Relationships between Hg(II)–S bond distance and Hg(II) coordination in thiolates, *Dalton Trans.*, 2008, 1421–1425.

64 O. Sénèque, P. Rousselot-Pailley, A. Pujol, D. Boturyn, S. Crouzy, O. Proux, A. Manceau, C. Lebrun, P. Delangle, Mercury trithiolate binding (HgS_3) to a de novo designed cyclic decapeptide with three preoriented cysteine side chains, *Inorg. Chem.*, 2018, **57**, 2705–2713.

65 S. Chakraborty, D. S. Touw, A. F. A. Peacock, J. Stuckey, V. L. Pecoraro, Structural comparisons of apo- and metalated three-stranded coiled coils clarify metal binding determinants in thiolate containing designed peptides, *J. Am. Chem. Soc.*, 2010, **132**, 13240–13250.

66 F. H. Allen, R. Mondal, N. A. Pitchford, J. A. K. Howard, Mapping the geometry of metal three-coordination using crystal structure data: Reaction pathway for ligand addition to linear Hg^{II} species, *Helv. Chim. Acta*, 2003, **86**, 1129–1139.

67 R. M. Gomila, A. Bauza, T. J. Mooibroek, A. Frontera, π-Hole spodium bonding in tri-coordinated Hg(II) complexes, *Dalton Trans*., 2021, **50**, 7545–7553.

68 D. Szunyogh, B. Gyurcsik, F. H. Larsen, M. Stachura, P. W. Thulstrup, L. Hemmingsen, A. Jancsó, Zn^{II} and Hg^{II} binding to a designed peptide that accommodates different coordination geometries, *Dalton Trans.*, 2015, **44**, 12576–12588.

69 M. Łuczkowski, M. Padjasek, J. B. Tran, L. Hemmingsen, O. Kerber, J. Habjanič, E. Freisinger, A. Krężel, An extremely stable interprotein tetrahedral $Hg(Cys)_4$ core forms in the zinc hook domain of Rad50 protein at physiological pH, *Chem. Eur. J.*, 2022, **28**, e202202738.

70 V. Arcisauskaite, S. Knecht, S. P. A. Sauera, L. Hemmingsen, Electric field gradients in Hg compounds: Molecular orbital (MO) analysis and comparison of 4-component and 2-component (ZORA) methods, *Phys. Chem. Chem. Phys.*, 2012, **14**, 16070–16079.

71 E. Freisinger, Spectroscopic characterization of a fruit-specific metallothionein: *M. acuminata* MT3, *Inorg. Chim. Acta*, 2007, **360**, 369–380.

72 G. R. Dieckmann, D. K. McRorie, D. L. Tierney, L. M. Utschig, C. P. Singer, T. V. O'Halloran, J. E. Penner-Hahn, W. F. DeGrado, V. L. Pecoraro, *De novo* design of mercury-binding two- and three-helical bundles, *J. Am. Chem. Soc.*, 1997, **119**, 6195–6196.

73 E. Mesterházy, C. Lebrun, S. Crouzy, A. Jancsó, P. Delangle, Short oligopeptides with three cysteine residues as models of sulphur-rich Cu(I)- and Hg(II)-binding sites in proteins, *Metallomics*, 2018, **10**, 1232–1244.

74 A. M. Pujol, C. Lebrun, C. Gateau, A. Manceau, P. Delangle, Mercury-sequestering pseudopeptides with a tris(cysteine) environment in water, *Eur. J. Inorg. Chem.*, 2012, 3835–3843.

75 S. Pires, J. Habjanič, M. Sezer, C. M. Soares, L. Hemmingsen, O. Iranzo, Design of a peptidic turn with high affinity for Hg^{II}, *Inorg. Chem.*, 2012, **51**, 11339–11348.

76 J. Chen, S. Sun, C.-Z. Li, Y.-G. Zhu, B. P. Rosen, Biosensor for organoarsenical herbicides and growth promoters, *Environ. Sci. Technol.*, 2014, **48**, 1141–1147.

77 Y. Sun, M. D. Wong, B. P. Rosen, Both metal binding sites in the homodimer are required for metalloregulation by the CadC repressor, *Mol. Microbiol.*, 2002, **44**, 1323–1329.

78 C. Eicken, M. A. Pennella, X. Chen, K. M. Koshlap, M. L. VanZile, J. C. Sacchettini, D. P. Giedroc, A metal–ligand-mediated intersubunit allosteric switch in related SmtB/ArsR zinc sensor proteins, *J. Mol. Biol.*, 2003, **333**, 683–695.

79 Y. Wang, L. Hemmingsen, D. P. Giedroc, Structural and functional characterization of *Mycobacterium tuberculosis* CmtR, a Pb^{II}/Cd^{II}-sensing SmtB/ArsR metalloregulatory repressor, *Biochemistry*, 2005, **44**, 8976–8988.

80 J. C. Payne, M. A. ter Horst, H. A. Godwin, Lead fingers: Pb^{2+} binding to structural zinc-binding domains determined directly by monitoring lead-thiolate charge-transfer bands, *J. Am. Chem. Soc.*, 1999, **121**, 6850–6855.

81 P. Rousselot-Pailley, O. Seneque, C. Lebrun, S. Crouzy, D. Boturyn, P. Dumy, M. Ferrand, P. Delangle, Model peptides based on the binding loop of the copper metallochaperone Atx1: Selectivity of the consensus sequence MxCxxC for metal ions Hg(II), Cu(I), Cd(II), Pb(II), and Zn(II), *Inorg. Chem.*, 2006, **45**, 5510–5520.

82 A. M. Pujol, C. Gateau, C. Lebrun, P. Delangle, A series of tripodal cysteine derivatives as water-soluble chelators that are highly selective for copper(I), *Chem. Eur. J.*, 2011, **17**, 4418–4428.

83 Gy. Szunyog, K. Várnagy, Lead(II) complexes of oligopeptides containing two cysteine residues, *Inorg. Chim. Acta*, 2018, **472**, 157–164.

84 H. Kaur, R. Kumar, J. N. Babu, S. Mittal, Advances in arsenic biosensor development – A comprehensive review, *Biosens. Bioelectron.*, 2015, **63**, 533–545.

85 B. Hajdu, A. Tóth, B. Fazekas, M. Horvát, K. Kato, A. Kawaguchi, K. Nagata, A. Jancsó, B. Gyurcsik, DNA recognition, cleavage, and toxic metal ion interaction of an artificial zinc finger protein inside E. coli cells, *Prot. Sci.,* 2026, (In production) 10.1002/pro.70599.

86 J. Aaseth, O. P. Ajsuvakova, A. V. Skalny, M. G. Skalnaya, A. A. Tinkov, Chelator combination as therapeutic strategy in mercury and lead poisonings, *Coord. Chem. Rev.*, 2018, **358**, 1–12.

87 G. Bjørklund, G. Crisponi, V. M. Nurchi, R. Cappai, A. B. Djordjevic, J. Aaseth, A review on coordination properties of thiol-containing chelating agents towards mercury, cadmium, and lead, *Molecules*, 2019, **24**, 3247.

88 A. M. Spuches, H. G. Kruszyna, A. M. Rich, D. E. Wilcox, Thermodynamics of the As(III)-thiol interaction: Arsenite and monomethylarsenite complexes with glutathione, dihydrolipoic acid, and other thiol ligands, *Inorg. Chem.*, 2005, **44**, 2964–2972.

89 S. Cavanillas, E. Chekmeneva, C. Ariño, J. M. Díaz-Cruz, M. Esteban, Electroanalytical and isothermal calorimetric study of As(III) complexation by the metal poisoning remediators, 2,3-dimercapto-1-propanesulfonate and meso-2,3-dimercaptosuccinic acid, *Anal. Chim. Acta*, 2012, **746**, 47–52.

90 J. S. Casas, M. M. Jones, Mercury(II) complexes with sulfhydryl containing chelating agents: Stability constant inconsistencies and their resolution, *J. Inorg. Nucl. Chem.*, 1980, **42**, 99–102.

91 X. Fang, F. Hua, Q. Fernando, Comparison of rac- and meso-2,3-dimercaptosuccinic acids for chelation of mercury and cadmium using chemical speciation models, *Chem. Res. Toxicol.*, 1996, **9**, 284–290.

92 D. K. Chakravorty, B. Wang, C. W. Lee, D. P. Giedroc, K. M. Merz, Jr., Simulations of allosteric motions in the zinc sensor CzrA, *J. Am. Chem. Soc.*, 2012, **134**, 3367–3376.

View Article Online
DOI: 10.1039/D6QI00870C

View Article Online
DOI: 10.1039/D6QI00876C

Data availability statement

The data supporting this article have been included as part of the Supplementary Information (ESI). Procedures of protein production including purification protocols, details of sample preparations, experimental methods and data fitting as well as figures and tables presenting spectral data and electrophoretic gel mobility shift assays are made available in the ESI. The code for the computer program PSEQUAD, used for the evaluation of equilibrium data, can be found at https://www.staff.u-szeged.hu/~peintler/enprogs.htm#psequad. The version of the code employed for this study is version 5.31.